An Optimal Feedback Approach to Particle Source Identification in Tokamaks

Enrique Santiago, Emmanuel Witrant, Marc Goniche, F. Clairet

An Optimal Feedback Approach to Particle Source Identification in Tokamaks

Enrique SANTIAGO*†, Emmanuel WITRANT*, Marc GONICHE† and Frédéric CLAIRET†
*GIPSA-lab, Université Joseph Fourier / CNRS, BP 46, 38 402 Saint Martin d'Hères, France
†CEA, IRFM, F-13108 Saint Paul-lez-Durance, France
Corresponding author: emmanuel.witrant@ujf-grenoble.fr

***Abstract*—A new identification technique is proposed to study the plasma phenomena taking place in the so-called *scrape-off layer* and their correlation with the *lower hybrid* radio frequency antenna in the experimental nuclear fusion tokamak reactor *Tore Supra*. A deeper knowledge of the plasma behavior in this region would contribute to the achievement of steady-state controlled thermonuclear fusion for power generation. The proposed approach relies on the design of a feedback/feedforward optimized architecture to solve a blind identification problem. While our paper is mostly focused on experimental results for the studied application, it can provide valuable insights on input estimation and model validation for transport phenomena described by partial differential equations.**

***Keywords:* distributed parameter systems, blind identification, process control.**

INTRODUCTION

Recent developments in control theory and controlled thermonuclear fusion research are naturally leading to research topics of common interest that are particularly challenging for both scientific communities. For example, new modeling and identification tools are needed for the understanding and analysis of complex physical phenomena. The representation (qualitative and quantitative) of particles transport at the plasma edge is an example of such topics.

Tokamak experiments, such as *Tore Supra* or *JET*, are equipped with Lower Hybrid (LH) antennas to heat the plasma and drive a non-inductive current. The LH waves are recognized as the most efficient non-inductive current drive sources and their use is forecasted for ITER experiment. A LHCD system has been implemented on Tore Supra since more than 20 years to fulfill the quasi-steady-state discharges objective [1] and has been proposed for ITER aiming at extending the pulse duration to 3000 s [2]. The efficiency of such antennas is strongly related to our ability to ensure an appropriate coupling between the waves on the plasma, which directly depends on the electron density in a region called the *scrape-off layer* (SOL), located between the last closed magnetic surface (the *separatrix*) and the wall. This region, as well as the key elements discussed in this work, are depicted in Figure 1. The importance of local density control in the SOL is emphasized in [3], [4].

The electron density in the SOL is directly influenced by the LH input power P_{LH} [3]. Indeed, a small but significant part of this power is absorbed in the plasma edge during the wave propagation to the core. A possible effect of this absorption

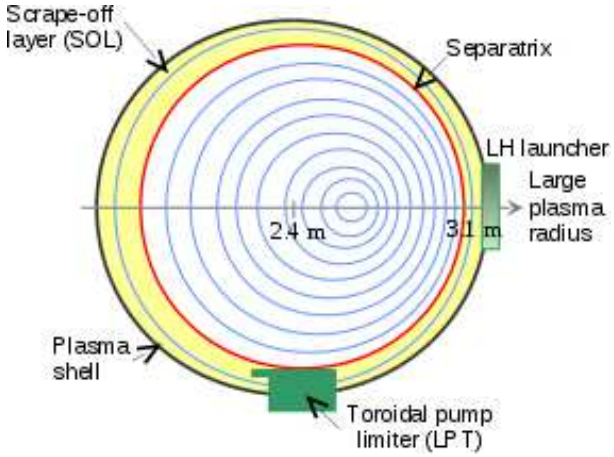

Fig. 1: Tore Supra cross section. Figure courtesy of [5].

is the gas ionization, which results in an increased electron density. This suggests that P_{LH} is a key parameter for the local control of the electron density, and consequently for the coupling efficiency. The development of new models based on experimental measurements that consider the impact of P_{LH} are consequently of prime interest. On Tore Supra, the electron density is measured by using a microwave reflectometer that has both a good spatial (≈ 1 *cm*) and temporal resolution (≈ 2 *ms* for the data considered).

The aim of this work is to propose an identification method for determining the *source term*, i.e. the number of electrons created per unit time and volume, when the high frequency heating is switched on. To achieve this, a simple particle transport model for the area of non-confined plasma (SOL) and a quasi-steady-state approach was proposed in [5]. Our aim is to develop an appropriate parametric identification method for distributed systems involving the transients, based on the reflectometer measurements. The resulting algorithm then provides an efficient tool for analyzing the coupling phenomena associated with the electron density behavior in the SOL, even if the detailed physical relationships are unknown.

This paper is organized as follows. First, the physical model and identification problem formulation are introduced in Section I. An optimal input identification procedure is then proposed in Section III, along with experimental results. The inclusion of shape constraints on the admissible inputs is

considered in Section IV. Finally, the physical transport model is revised with a multizone approach in Section V.

I. Physical model and problem formulation

Using specific hypotheses associated with the physical properties of the SOL, the following transport model was established in [5]:

$$\frac{\partial \tilde{n}_e}{\partial t} = D_\perp(t)\frac{\partial^2 \tilde{n}_e}{\partial r^2} - \frac{\tilde{c}_s(r,t)}{2\tilde{L}_c(r,t)}\tilde{n}_e + \tilde{s}(r,t) \tag{1}$$

where $n_e(r,t)$ is the electron density, r is the small plasma radius, t is the time, $D_\perp$ is the cross-field diffusion coefficient (typically $\sim 1\ m^2 s^{-1}$, which is the value used for the presented simulations), c_s the sound speed, L_c the connecting length along the flux tube to the flow stagnation point and $\tilde{s} = S_{LPT} + S_{LH}$ reflects the particle source induced by the pumped toroidal limiter S_{LPT} and the LH antenna S_{LH}. The tilde superscript denotes the expression of the variables in terms of the tokamak small radius and will be dropped in the remaining of the paper after the radius normalization. The sound speed can be approximated as $c_s \approx \sqrt{(T_e + T_i)/m_i}$, where T_e and T_i are the electron and ion temperatures, and m_i is the ion mass. The ratio T_i/T_e is obtained thanks to the experimental measurements described in [6]. In the case of a toroidal limiter, $\tilde{L}_c$ is deduced from the safety factor q as $\tilde{L}_c \approx 2\pi R_0 q$, where R_0 is the plasma major radius. When no other objects (chamber wall, secondary limiters…) intercept the field lines in the SOL, this connection length has small variations and will be considered as constant.

A Neumann boundary condition $\partial \tilde{n}_e(0,t)/\partial r = 0$ is set at the center while a Dirichlet one $\tilde{n}_e(L,t) = n_{e,L}(t)$, where $n_{e,L}(t)$ is given by the measurements, governs the plasma edge. The data set considered in this paper is characterized by constant and repeated LH impulses that highlight the impact of LH antenna (no other radio frequency source).

As a first approach, this paper is focused on determining the variations of the source term $\tilde{s}(r,t)$ in (1) from the measurements of $\tilde{n}_e(r,t)$. The transport parameters $D_\perp$, $\tilde{c}_s$ and $\tilde{L}_C$ are obtained from existing models and measurements. They are assumed to be constant according to a supposed steady state behavior of the plasma transport properties (i.e. these parameters vary slowly in comparison with the state dynamics).

Using the subscripts t and z to denote the time and space derivatives, respectively, where $z = r/L \in [0,\ 1]$ is the normalized radius, the class of systems considered can be described as:

$$\begin{cases} n_{e,t}(z,t) = \alpha\, n_{e,zz}(z,t) - \nu\, n_e(z,t) + s(z,t), \\ n_{e,z}(0,t) = n_{e,z0}(t), \quad n_e(1,t) = n_{e,L}(t), \\ n_e(z,0) = n_{e,t0}(z), \end{cases} \tag{2}$$

where $\alpha = D_\perp/L^2$ is the diffusion and $\nu = c_s/(2L_C) > 0$ is the sink term. The existence and unicity of a solution can be proved with the results proposed by [7].

The dynamics (2) can be approximated by ordinary differential equations by discretizing with respect to space (see [8] or similar textbooks for a detailed analysis of the discretization step). For example, the finite differences method with a central discretization of the diffusion term:

$$\frac{\partial^2 n_e}{\partial z^2} \approx \frac{n_{e,i+1} - 2n_{e,i} + n_{e,i-1}}{\Delta z^2}$$

where $n_{e,i}(t)$ denotes the value of $n_e(z,t)$ at the location $z = z_i$ ($i = 1,\ \cdots, N$, where N is the number of measurements), and the use of the boundary conditions as:

$$n_{e,z}(0,t) \approx \frac{n_{e,1}(t) - n_{e,0}(t)}{\Delta x} = n_{e,z0}(t), \quad n_{e,N+1} = n_{e,L}(t),$$

provides a N-dimensional state-space model of the density distribution. It writes in the standard state-space form:

$$\dot{x} = Ax + BS + w, \quad x(0) = x_0$$

where $x = [n_{e,1}\ n_{e,2}\ \cdots\ n_{e,N}]^T$, $S = [s_1\ s_2\ \cdots\ s_N]^T$, $w = [a_1 n_{e,z0}\ 0\ \cdots\ 0\ a_2 n_{e,L}]^T$, $a_{1,2}$ are coefficients determined by the spacial discretization scheme, $A \in \mathbb{R}^{N\times N}$ (see [9] for a complete description of the matrix elements and $a_{1,2}$) and $B = I \in \mathbb{R}^{N\times N}$.

II. A feedback approach to blind identification

Classical identification methods are available to determine the system behavior (or specific parameters) based on input/output data. Our problem is slightly different as the term that has to be identified is the input variable itself (the so-called source term). This relates to specific research issues, typically considered from the signal processing point of view and referred to as *blind identification problems* (see for example [10], [11] and references therein). This designation alludes to the fact that we don't have information about the input that is being introduced in the system.

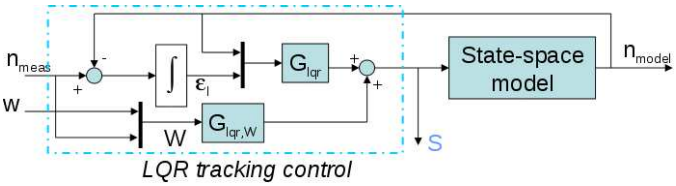

Fig. 2: Optimal tracking for blind identification.

An alternative to the signal processing approach is to formulate an optimal tracking problem based on the model and the measurements [12]. In this case, the model is the system which dynamics has to be controlled, $S(t)$ acts as the controlled input and the measurement $n_{e,meas}(t)$ is the tracked reference. The control objective is thus to minimize the modeling error $\varepsilon(t) = n_{e,meas}(t) - n_{e,model}(t)$ over the experiment time horizon. It can be achieved for example using a LQR tracking controller with integral action. This specific architecture is presented in Figure 2. The related control law is detailed in the next section.

III. Optimal source identification

The aim of this section is to design an optimal approach to the source identification, considering a given transport model and a density measurements data set. The proposed optimization method is inferred from the variational approach to optimal control problems, such as the one described in [13].

A. Extended state and cost function

An integral action is first introduced in the feedback architecture by extending the state with a new variable corresponding to the integral of the estimation error $\varepsilon(t)$. The estimation error is the difference between the reference signal r (e.g. the measured plasma density) and the model output $y = x$ (e.g. the modeled plasma density). The extended state writes as:

$$\underbrace{\frac{d}{dt}\begin{bmatrix} x \\ \varepsilon_I \end{bmatrix}}_{\dot{X}} = \underbrace{\begin{bmatrix} A & 0 \\ -I & 0 \end{bmatrix}}_{A_e}\underbrace{\begin{bmatrix} x \\ \varepsilon_I \end{bmatrix}}_{X} + \underbrace{\begin{bmatrix} B \\ 0 \end{bmatrix}}_{B_e} S + \underbrace{\begin{bmatrix} w \\ r \end{bmatrix}}_{W} \tag{3}$$

Our aim is to optimize the estimated source such that ε should be close to zero with a minimum weighted input effort. The cost function that is to be minimized is consequently:

$$J = \frac{1}{2}\int_0^{t_f} \begin{bmatrix} \mathrm{x} \\ \varepsilon_I \end{bmatrix}^T \begin{bmatrix} 0 & 0 \\ 0 & Q_r \end{bmatrix} \begin{bmatrix} \mathrm{x} \\ \varepsilon_I \end{bmatrix} dt + S^T R\, S\, dt \tag{4}$$

where $Q_r = Q_r^T \geq 0$ weights the integrated error and $R = R^T > 0$ the input usage.

B. Optimal tracking with exogenous inputs

The Hamiltonian associated with (3)-(4) writes as:

$$H = \tfrac{1}{2}(\varepsilon_I^T Q_r \varepsilon_I + S^T R S) + \lambda^T (A_e X + B_e S + W) \tag{5}$$

where λ denotes the Lagrange multipliers (adjoint state). The optimal input is given by the following necessary condition

$$\frac{\partial H}{\partial S} = RS + B_e^T \lambda = 0 \Leftrightarrow S = -R^{-1} B_e^T \lambda \tag{6}$$

The adjoint vector $\lambda(t)$ is solution of the differential equation:

$$\dot{\lambda} = -\frac{\partial H}{\partial X} = -A_e^T \lambda(t) - Q_r X \tag{7}$$

It can be shown (considering the extended system composed of X and λ) that a general solution to the previous equation writes as:

$$\lambda(t) = P(t)X(t) - \gamma(t) \tag{8}$$

where $P(t)$ and $\gamma(t)$ are real variables of appropriate dimensions. Expressing (7) in terms of the previous solution implies:

$$\dot{\lambda}(t) = (-A_e^T P - Q_r)X + A_e^T \gamma \tag{9}$$

Introducing (6) and (8) into (3) gives the optimal state trajectory:

$$\begin{aligned} \dot{X} &= A_e X - B_e R^{-1} B_e^T \lambda + W \\ &= A_e X - B_e R^{-1} B_e^T P X + B_e R^{-1} B_e^T \gamma + W \end{aligned} \tag{10}$$

The differential equation (7) can now be written as

$$\begin{aligned} \dot{\lambda}(t) &= \dot{P}(t)X(t) + P(t)\dot{X}(t) - \dot{\gamma}(t) \\ &= (\dot{P} + PA_e - PB_e R^{-1} B_e^T P)X + (PB_e R^{-1} B_e^T)\gamma \\ &\quad + PW - \dot{\gamma} \end{aligned} \tag{11}$$

Equating (9) and (11) provides:

$$\begin{aligned} \dot{P} &= PB_e R^{-1} B_{e\,e}^T P + Q_r - PA_e - A_e^T P \\ \dot{\gamma} &= PB_e R^{-1} B_e^T \gamma + PW - A_e^T \gamma \end{aligned} \tag{12}$$

Which allows for the computation of the optimal source given by (6). The boundary of the previous dynamics are provided by the terminal constraints $P(t_f) = 0$ and $\gamma(t_f) = 0$ (as no terminal cost is considered in J).

Supposing that γ and P reach equilibrium with limited variations (infinite horizon solution), a quasi-steady state solution can be used for simplified computations with:

$$\begin{aligned} Q_r &= PA_e + A_e^T P - PB_e R^{-1} B_e^T P \\ \gamma(t) &= -[PB_e R^{-1} B_e^T - A_e^T] P W(t) \end{aligned} \tag{13}$$

The optimal state trajectory is then given by:

$$\dot{X}(t) = A_e X - B_e R^{-1} B_e^T P X + B_e R^{-1} B_e^T \gamma(t) \tag{14}$$

and the corresponding optimal input is:

$$u(t) = -R^{-1} B_e^T [PX(t) - \gamma(t)] \tag{15}$$

with P and γ provided either by (12) or (13). Simulations tests comparing the use of the dynamic or the quasi-steady-state solutions for P and γ have shown that both were equivalent. The quasi-steady-state solution is preferred and kept in the final design, as it is simpler to implement. The optimal input thus has a feedback (Riccati equation) plus feedforward (to include time-variations of the boundary conditions) architecture. The controller gains presented on Figure 2 are thus:

$$G_{lqr} = -R^{-1} B_e^T P, \quad G_{lqr,W} = -R^{-1} B_e^T [PB_e R^{-1} B_e^T - A_e^T] P$$

C. Structure verification and Q_r and R tuning

To test the performance of the structure, a verification test was carried out with physical values for the transport parameters. Inserting an hypothetical Gaussian particle source $S(t)$ in the model, a theoretical density distribution $x(t)$ was obtained. This distribution was introduced in the identification structure and the Gaussian source was retrieved. The identification efficiency is evaluated thanks to the normalized accumulated tracking error:

$$\bar{e}(t) = \Delta z \sum_{i=0}^{N} e_i(t), \text{ with } e(t) = \left| \frac{x_{measured}(t) - x_{model}(t)}{x_{model}(t)} \right|$$

where e_i is the i^{th} component of e. When the weighting matrices for the LQR are chosen as $Q_r = R = I$, it was noticed that the estimation error, although small, was always persistent. Since an integral action had been added to the system, the steady state error is expected to disappear relatively quickly. As the plasma/wave coupling phenomenon is quasi-instantaneous (in comparison with the density time constant), the estimation settling time needs to be much faster than the

system dynamics, which was achieved by setting $Q_r = 10^7 \times I$ and $R = 10^{-7} \times I$. The associated simulation results can be found in [9].

D. Application to real data shot TS38953

The adequacy of the proposed method to model experimental results is investigated on Tore Supra density measurements from shot TS38953. In this shot, the LH antenna was being constantly switched on and off. The boundary conditions are first supposed to be constant with $n_{ez0}(t) = n_{e,L}(t) \equiv 0$ (this hypothesis will be released in the next section). Figure 3 presents the measured density and the accumulated tracking error. The identified source term can be observed in Figure 4a.

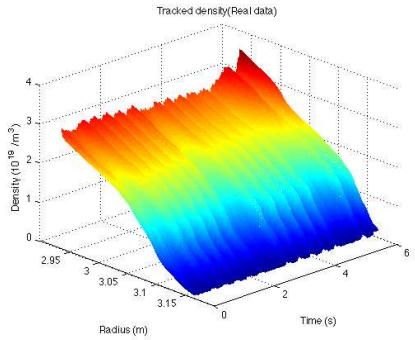

(a) Measured density

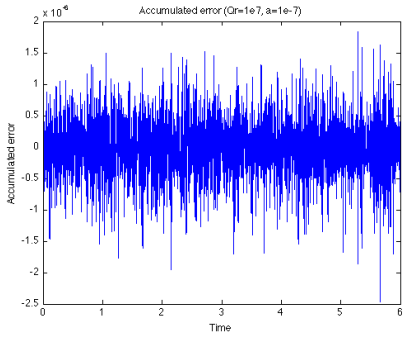

(b) Accumulated tracking error $\bar{e}(t)$

Fig. 3: Measured density and accumulated tracking error from TS38953.

As expected, two sources appear in the SOL, one due to the limiter (LPT) and the other one due to the LH antenna. The source term can thus be written as:

$$S(z,t) = S_{LPT}(z,t) + S_{LH}(z,t)$$

where $S_{LPT}(z,t)$ is larger than $S_{LH}(z,t)$. Also, a plasma displacement when the LH power is on can be observed (non-uniform normalized plasma radius with respect to the sensors frame).

While the low accumulated error is satisfactory, three main problems appear:

1) the source term reaches negative values, which cannot happen in the real source term;
2) positive values reached by the source are much higher than it was expected (increased by 10^2);
3) edge distortion appears in the source due to the constant boundary conditions that had been chosen in the initial design.

Specific strategies (such as anti-windup or saturations) can be used to solve the positivity problem. Nevertheless a revision of the transport model is preferred, in order to provide a feedback on the physical phenomena understanding. The three main problems are discussed in the following sections.

E. Time varying boundary conditions

To solve the edge source distortion problem, time varying boundary conditions were added and taken into account with the feedforward term $\gamma(t)$. The new identified source term is presented on Figure 4b: the edges are no longer distorted. On the other hand, the inner part if the source distribution doesn't suffer substantial changes and the order of magnitude for the density accumulated tracking error is maintained as 10^{-6}.

F. Application to real data shot TS45525

Due to the abnormal amplitude obtained with data shot TS38953, we decided to try the structure with another data shot obtained from Tore Supra, the shot TS45525. This shot, unlike the first one, was obtained using constant LH heating power. This allows for decoupling the electron density transport phenomena from the complex plasma-wave interactions and the plasma shape variations. The related identified source profile is presented on Figure 5.

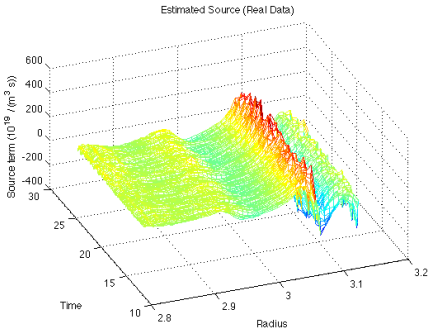

Fig. 5: Unconstrained identified source for TS45525.

It can be observed that, even if negative values keep appearing in the source term, the order of magnitude of the sources is around the expected one. Further studies will consequently be needed to identify the cause of the high source term obtained when the LH power changes abruptly, eventually including a refined model to depict the transients associated with the plasma-wave interactions.

In the new source term, a third peak can be observed between the LPT and LH sources. This third source can be caused by the antenna protection limiter (LPA) that was not taken off during TS45525 (unlike in TS38953, where it was removed especially for that experience). In fact, the

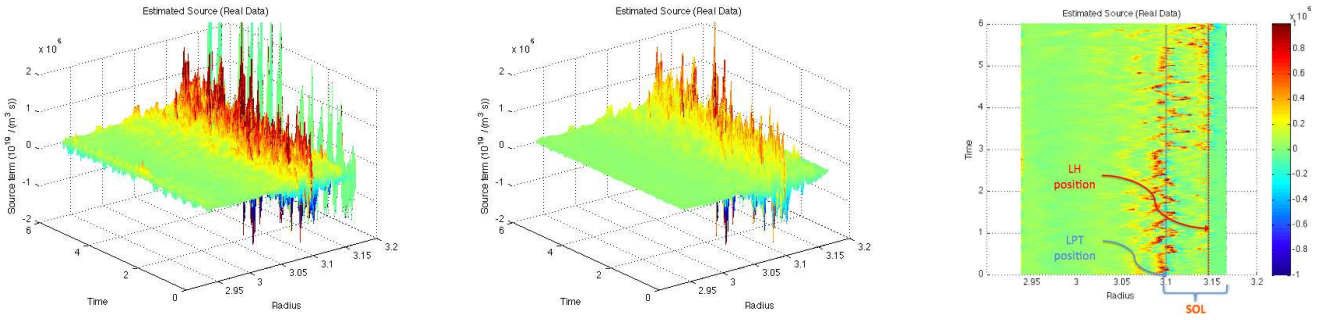

(a) With constant boundary conditions (b) With time-varying boundary conditions (c) Top view of the identified source

Fig. 4: Identified source term for TS38953.

position of the plasma facing components during this shot were: LPT at $R = 3.086\,\text{m}$, LPA at $R = 3.116\,\text{m}$ and LH at $R = 3.153\,\text{m}$. These values correspond approximately with the source peak positions observed on the identified term. We can thus conclude that the new obtained source is more coherent with the expected values. Nevertheless, the source term in the confined plasma always presents positive values (though small), while it should be zero in this region. This problem will be solved by a multi-zone approach in Section V.

IV. Constrained optimal identification

With the aim of avoiding negative values in the source term, a constrained identification structure was designed so that a determined shape could be imposed to the input source term. In this section, the deduced constrained system and the constrained equilibrium source are first introduced. Then, the designed constrained identification structure and the numerical issues observed during its application to the real system are exposed.

A. Constrained system and equilibrium Gaussian source term

From [5], the assumption of a SOL source term composed by two Gaussian distributions (one due to the LPT and the other one due to the LH antenna) was taken. The main idea consists in changing the arbitrary distributed input source for a Gaussian shaped distributed source parameterized by the amplitude $\theta(t)$, the mean $\mu(t)$ and the standard deviation $\sigma(t)$ of the two Gaussian distributions:

$$s(z,t) = \theta_{LPT} e^{-(z-\mu_{LPT})^2/(2\sigma_{LPT}^2)} + \theta_{LH} e^{-(z-\mu_{LH})^2/(2\sigma_{LH}^2)}$$

The associated constrained discretized input is consequently set with:

$$S_i(t) = \sum_{j=\{LPT,LH\}} \theta_j(t) e^{-(z_i-\mu_j(t))^2/(2\sigma_j(t)^2)}$$

The unconstrained source input is thus replaced by a nonlinear (Gaussian) function of the parameters:

$$\vartheta(t) = [\theta_{LPT}\ \ \mu_{LPT}\ \ \sigma_{LPT}\ \ \theta_{LH}\ \ \mu_{LH}\ \ \sigma_{LH}]^T$$

In order to include the nonlinearity in ϑ in the proposed optimization framework, it has to be linearized (first order approximation) around an equilibrium point (denoted with the subscript eq).

The parameters ϑ_{eq} for the Gaussian equilibrium source are computed such that the averaged error between the obtained density and the measured density is minimized. The corresponding data set $\{x_{eq}, w_{eq}\}$ is selected to correspond to time instants when LH is on and the profiles are stabilized, and the source parameters are obtained by solving the optimization problem:

$$\vartheta_{eq} = arg\min_{\vartheta} \left\{ Ax_{eq} + \nabla_{\vartheta} S|_{\vartheta_{eq}}\, \vartheta + w_{eq} \right\}$$

where $\nabla_{\vartheta} S|_{\vartheta_{eq}}$ denotes the partial derivative of S with respect to ϑ (Jacobian operator), evaluated at ϑ_{eq}. The obtained equilibrium source and the equilibrium density are presented in Figure 6. This source represents the optimal constrained (Gaussian like) input for the system in order to obtain the equilibrium density, taken as the mean density.

B. Numerical difficulties

Once the system was linearized around the equilibrium source, a constrained identification structure was designed to obtain the Gaussian-like source term varying in time. This structure would retrieve the incremental Gaussian parameters (the input to the linearized constrained system) and calculate the corresponding Gaussian shaped source.

Unfortunately, although the performance of this identification structure was verified with more simple systems, when the system under study (the constrained linearized input system) was implemented, numerical problems took place and the solution for the LQR optimal controller could not be found. After studying this situation, we arrived to the conclusion that the difficulty lied in solving the Riccati equation. To solve this sort of equations, we used the *Matlab*® function *care* (the one used to obtain the optimal controller in the unconstrained structure), which computes the eigenvalues of the Hamiltonian matrix:

$$\mathscr{H} = \begin{pmatrix} A_e & -B_e R^{-1} B_e^T \\ -Q_r & -A_e^T \end{pmatrix}$$

For the constrained case, *Matlab*® justifies that the eigenvalues of this matrix are too near to the imaginary axis, and

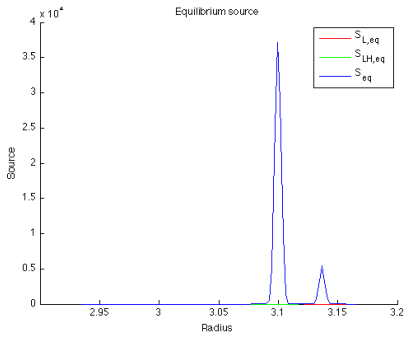

(a) Equilibrium Gaussian source

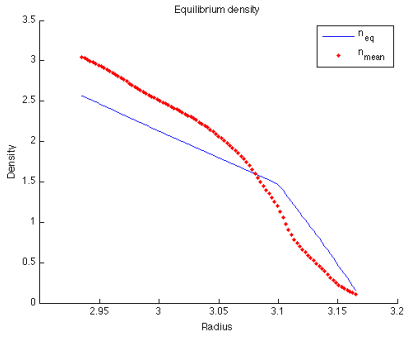

(b) Corresponding equilibrium density and mean density

Fig. 6: Optimal equilibrium Gaussian source and density.

thus, it cannot find the solution to the Riccati equation. This problem mainly comes from the fact that A_e is not full rank and can be corrected, for example, by adding a forgetting factor on the integrated error (negative term in the lower right part of A_e). This has been successfully implemented in [14].

V. A MULTIZONE APPROACH

The previous sections have been focused in achieving the most accurate SOL identification structure in order to retrieve a source term with an expected shape. This section is focused on revising the SOL model with radial anisotropy. A new SOL model based on three different regions is thus proposed.

A. Compartmental description with a 3-zones model

The limitations highlighted in the previous sections (higher source values during transients and negative identified terms) motivate the need for a more complex and accurate transport model of the SOL. Indeed, [15] suggests that an advection model may be more appropriate for the last part of the SOL. In addition, for the plasma placed before the separatrix (e.g. confined plasma), there would be no sink term since the magnetic field lines in confined plasma are closed on themselves. The edge plasma region is thus split into three different subregions (see Figure 7): the confined plasma, first part of SOL and final part of SOL. We consequently have the following transport models:

- Diffusion model (in the confined plasma region):

$$n_{e,t} = D_\perp n_{e,zz} + S(z,t) \tag{16}$$

- Diffusion model with sink term (in the first part of non confined plasma region or SOL):

$$n_{e,t} = D_\perp n_{e,zz} - \nu n_e(z,t) + S(z,t) \tag{17}$$

- Advection model with sink term (in the second part of the SOL):

$$n_{e,t} + V_c n_{e,z} = -\nu n_e(z,t) + S(z,t) \tag{18}$$

with continuity conditions (Neumann boundaries) between each zone. The specific computation of the transport parameters in each zone can be found in [9].

To integrate these three models in the same state-space representation, the following generic description is used:

$$\begin{cases} n_{e,t} = D(z)n_{e,zz} + V(z)n_{e,z} + R(z)n_e + S(z,t), \\ n_{e,z}(0,t) = n_{e,z0}(t), \quad n_e(1,t) = n_{e,L}(t), \\ n_e(z,0) = n_{e,t0}(z), \end{cases} \tag{19}$$

where D, V and R are evaluated at each location z_i and set according to the descriptions (16)-(18). To delimit the different regions, two points are defined:

- $\mathbf{n_a}$ marks the end of confined plasma and thus the beginning of the SOL. It is chosen around the separatrix or LCMS (the position of the LCMS can be retrieved from the TS database for each shot);
- $\mathbf{n_b}$ marks the beginning of the advection model in the SOL (around 4 cm after the LCMS).

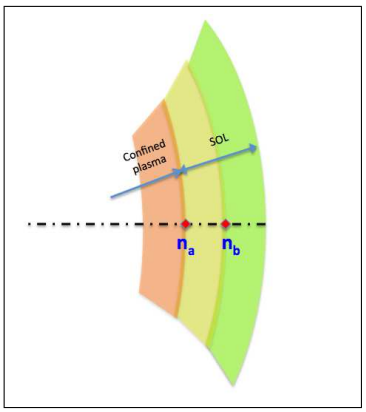

Fig. 7: Subregions in edge plasma.

B. Parameters computation and obtained source term

The space parameters are set according to the zones definition as depicted in Figures 8a-8b for the data shot TS45525. The related algorithm was conceived to allow space-varying parameters for the models, which is a more realistic situation than the constant-parameter case. Figure 8c presents the obtained source term (almost constant as the LH power input was constant for TS45525).

Comparing these results with the ones obtained with the first estimation structure (see Figure 5), it can be observed that the negative values have been reduced and the values for the three sources that keep appearing are more consistent with

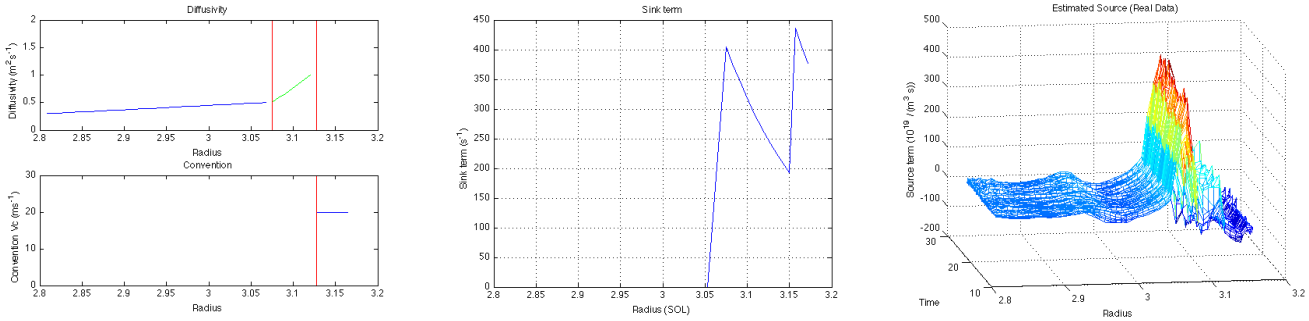

(a) Values for the $D \perp$ and the Vc coefficients

(b) Values for the sink term

(c) Source profile

Fig. 8: Calculated parameters and resulting source term for TS45525 using the 3 zones model.

the expected values. Also, it can be seen that the source term in confined plasma is almost zero. The new model thus appears to be more accurate in terms of the qualitative representation of the expected physical phenomena and of the expected source amplitude.

It is important to notice that the obtained source term is very sensitive to variations in the model parameters, which hints towards future research focused on the estimation robustness and the estimation of time-varying transport parameters.

Conclusions

In this paper, we have developed an optimal feedback approach to infer a time-varying input for a system model when the output is measured. While this structure has been developed for the SOL model in tokamaks, it can easily be extrapolated to other systems characterized by (possibly anisotropic) transport phenomena. This identification method makes possible the use of constraints on the input or models with multiple interconnected regions. Experimental results have shown the effectiveness and limitations of the proposed approach.

Future research will focus on the specificity associated with the identification of sources with fast varying parameters and combined source/transport parameters estimation.

Acknowledgments

The authors are grateful to the anonymous reviewers, who provided numerous insights for the paper improvement and to motivate further research on this topic. This work, supported by the European Communities under the contract of Association between EURATOM and CEA, was carried out within the framework of the European Fusion Development Agreement. The views and opinions expressed herein do not necessarily reflect those of the European Commission. The Tore Supra LHCD team is acknowledged for operating the LHCD system.

References

[1] A. Ekedahl, M. Goniche, D. Guilhem, F. Kazarian, Y. Peysson, and Tore Supra Team, "Lower hybrid current drive in tore supra," *Fusion Science and Technology*, vol. 56, no. 3, pp. 1150–1172, Oct. 2009.

[2] G. Hoang *et al.*, "A lower hybrid current drive system for iter," *Nuclear Fusion*, vol. 49, no. 7-075001, 2009.

[3] J. Mailloux *et al.*, "Long distance coupling of the lower hybrid waves on Tore Supra," in *Proc. of the* 25^{th} *Eur. conf. on Cont. Fus. and Plasma heating*, 1998.

[4] A. Ekedahl *et al.*, "Long distance coupling of lower hybrid waves in JET plasmas with edge and core transport barriers," *Nucl. Fusion*, 2005.

[5] E. Witrant, M. Goniche, and Equipe TORE SUPRA, "A qss approach for particle source identification in tore supra tokamak," in *Proc. of 48th IEEE Conference on Decision and Control*, Shanghai, Dec. 2009.

[6] M. Kočan, J. Gunn, J.-Y. Pascal, G. Bonhomme, C. Fenzi, E. Gauthier, and J.-L. Segui, "Edge ion-to-electron temperature ratio in the Tore Supra tokamak," *Plasma Phys. Control. Fusion*, vol. 50, pp. 125 009–125 019, 2008.

[7] A. Pazy, *Semigroups of Linear Operators and Applications to Partial Differential Equations*, ser. Applied mathematical sciences. New York: Springer Verlag, 1983, vol. 44.

[8] G. Allaire, *Numerical Analysis and Optimization: An Introduction to Mathematical Modelling and Numerical SImulation*, 9th ed. New York: Oxford Univ. Press, 2007.

[9] E. Santiago, "Particle source identification in the plasma edge in tore supra tokamak," Master's thesis, Université de Grenoble, 2010.

[10] S. Achard, D. Pham, and C. Jutten, "Criteria based on mutual information minimization for blind source separation in post nonlinear mixtures," *Signal Processing*, vol. 85, no. 5, pp. 965–974, 2005, special issue on Information Theoretic Signal Processing.

[11] Y. Yu and A. Petropulu, "Parafac-based blind estimation of possibly underdetermined convolutive mimo systems," *IEEE Transactions on Signal Processing*, vol. 56, no. 1, pp. 111–124, 2008.

[12] J. Weydert, "Source determination in non-homogeneous dissipative media," Master's thesis, University Joseph Fourier, 2009.

[13] D. Kirk, *Optimal Control Theory: An Introduction*, ser. Electrical engineering. Englewood Cliffs, New Jersey: Prentice-Hall, 1970.

[14] F. Bribiesca Argomedo, E. Witrant, C. Prieur, D. Georges, and S. Brémond, "Model-based control of the magnetic flux profile in a tokamak plasma," in *Proc. of 49th IEEE Conference on Decision and Control*, Atlanta, USA, Dec. 2010.

[15] X. Garbet, "Plasma edge physics," Association Euratom-CEA, CEA/DSM/DRFC, CEA-Cadarache, France, lecture notes for the master Sciences de la Fusion, Oct. 2008.